

# The Type Ib SN 1999dn: One Year of Photometric and Spectroscopic Monitoring. <sup>\*</sup>

S. Benetti,<sup>1†</sup> M. Turatto,<sup>2</sup> S. Valenti,<sup>3</sup> A. Pastorello,<sup>3</sup> E. Cappellaro,<sup>1</sup> M.T. Botticella,<sup>3</sup> F. Bufano,<sup>1</sup> F. Ghinassi,<sup>4</sup> A. Harutyunyan,<sup>4</sup> C. Inserra,<sup>2</sup> A. Magazzù,<sup>4</sup> F. Patat,<sup>5</sup> M.L. Pumo,<sup>2</sup> S. Taubenberger<sup>6</sup>

<sup>1</sup>*Osservatorio Astronomico di Padova, vicolo dell'Osservatorio 5, I-35122, Padova, Italia*

<sup>2</sup>*Osservatorio Astrofisico di Catania, Via S. Sofia 78, I-95123, Catania, Italia*

<sup>3</sup>*Astrophysics Research Centre, School of Mathematics and Physics, Queen's University Belfast, BT7 1NN, UK*

<sup>4</sup>*Telescopio Nazionale Galileo, Fundación Galileo Galilei - INAF, Rambla José Ana Fernández Pérez, 7, 38712 Breña Baja, TF - Spain*

<sup>5</sup>*European Southern Observatory, Karl Schwarzschild-Str. 2, 85748, Garching bei München, Germany*

<sup>6</sup>*Max-Planck-Institut für Astrophysik, Karl Schwarzschild Str. 1, 85741 Garching bei München, Germany*

Received .....; accepted .....

## ABSTRACT

Extensive optical and near-infrared (NIR) observations of the type Ib supernova 1999dn are presented, covering the first year after explosion. These new data turn this object, already considered a prototypical SNIb, into one of the best observed objects of its class. The light curve of SN 1999dn is mostly similar in shape to that of other SNIb but with a moderately faint peak ( $M_V = -17.2$  mag). From the bolometric light curve and ejecta expansion velocities, we estimate that about  $0.11M_\odot$  of  $^{56}\text{Ni}$  were produced during the explosion and that the total ejecta mass was  $4 - 6M_\odot$  with a kinetic energy of at least  $5 \times 10^{51}$  erg. The spectra of SN 1999dn at various epochs are similar to those of other Stripped Envelope (SE) SNe showing clear presence of H at early epochs. The high explosion energy and ejected mass, along with the small flux ratio  $[\text{CaII}]/[\text{OI}]$  measured in the nebular spectrum, together with the lack of signatures of dust formation and the relatively high-metallicity environment point toward a single massive progenitor ( $M_{\text{ZAMS}} \geq 23 - 25 M_\odot$ ) for SN 1999dn.

**Key words:** Supernovae and Supernova Remnants: general – Supernovae and Supernova Remnants: 1999dn

## 1 INTRODUCTION

In the Supernova (SN) taxonomy, type Ib Supernovae (SNIb) are defined as the subclass of Core-Collapse explosions (CC-SNe) whose early-time spectra are characterized by strong HeI lines (e.g. Wheeler & Levreault 1985; Turatto, Benetti, & Pastorello 2007). CC-SNe are thought to descend from massive progenitors ( $M > 7 - 8 M_\odot$ ) and include also the most frequent, H-dominated type II SNe (SNII) as well as type Ic SNe (SNIc), which appear deprived of both H and He. The physical connection among these subtypes is provided by their location almost exclusively in spiral galaxies

(e.g. Hakobyan et al. 2008) and, in particular, by their association to massive star formation regions (e.g. Van Dyk et al. 1999; Anderson & Jones 2008). An additional evidence of a link between the different subtypes of CCSNe came with the discovery of objects, called type IIb, that metamorphose from type II at early stages to type Ib later on. The prototype of this subclass is SN 1993J in M81, one of the best studied SNe at all wavelengths ever (e.g. Barbon et al. 1995; Richmond et al. 1996b).

While early time spectra of CC-SNe can be very different as a consequence of the different configurations of the progenitors at the moment of their explosions, late time spectra of all CC-SNe are consistently similar with strong emission lines of neutral and singly ionized O and Ca, in addition to H Balmer lines for SNII. The standard scenario is that SNIb descend from massive stars that have lost their H envelope through strong winds or mass transfer to a companion (Heger et al. 2003). If in addition to the H also the He envelope has been removed, then the SN will appear of

<sup>\*</sup> Based on observations collected at the European Organisation for Astronomical Research in the Southern Hemisphere, Chile (ESO programmes 64.H-0604 and 65.H-0292), at the Italian 3.58m Telescopio Nazionale Galileo and the William Herschel Telescope (La Palma, Spain), and at the Copernico telescope (Asiago, Italy).

<sup>†</sup> E-mail: stefano.benetti@oapd.inaf.it

type Ic. For this reason SNIb, Ic and IIb are often referred to as Stripped Envelope (SE) SNe.

With the improved quality of data, the differences between type Ib and Ic have shown to be subtle, and classifications often controversial. For instance, in SN 1994I, early on considered as the prototypical SNIc, has been found **possible** signature of He (Filippenko et al. 1995; Clocchiatti et al. 1996); the type Ib SN 1999ex was characterized by weak optical HeI but strong HeI  $\lambda 10830$ ,  $\lambda 20581$  lines in the near-IR (Hamuy et al. 2002); the peculiar SN 2005bf (Folatelli et al. 2006) and SN 2008D (Mazzali et al. 2008; Modjaz et al. 2009) underwent a metamorphosis from a broad line type Ic at early times to a typical type Ib at later epochs. The sharp distinction between the two classes seems therefore to be replaced by a continuity of properties in He abundances and/or excitation.

The study of stripped-envelope SNIb/c has received fresh impetus in the past decade because of the association of some of them, in particular the most energetic SNIc (hypernovae), with GRBs of long duration (Galama et al. 1998; Hjorth et al. 2003; Malesani et al. 2004). More recently a few SNIc have been associated with less energetic X-ray flashes (Fynbo et al. 2004; Modjaz et al. 2006; Pian et al. 2006). An X-ray flash was also detected in the type Ib, which was attributed either to shock break-out at the star surface (Soderberg et al. 2008) or to the effect of mildly relativistic jets due to the collapse of a  $30 M_{\odot}$  star to a black hole (Mazzali et al. 2008).

Despite this renewed interest the objects with detailed observations remain few. In particular, it is not well ascertained if SNIb do exist as a distinct class or if there is a uniform distribution of objects from SNII to SNIc with decreasing H (and He) content in the outer layers. In this context, SN 1999dn is interesting because it has been adopted several times in the past to describe the average properties of SNIb (e.g. Branch et al. 2002; Chornock et al. 2010).

SN 1999dn was discovered by Qiu et al. (1999a) on two unfiltered CCD images obtained on Aug. 19.76 and 19.82 UT, respectively, in the Wolf-Rayet galaxy NGC 7714. The SN position is R.A.(2000.0)= $23^h36^m14^s.7$ ; Dec(2000.0)= $+02^{\circ}09'08''.8$ ,  $9.9''E$ ,  $9.4''S$  of the galaxy nucleus (Qiu et al. 1999a), in a region of steep background variation (Fig. 1). The parent galaxy, NGC 7714, is classified as SBB peculiar, and identified by Weedman et al. (1981) as a prototypical starburst galaxy. A second SN (2007fo), has been recently discovered  $2.5''W$ ,  $12.4''N$  of the galaxy nucleus (Khandrika & Li 2007), which showed similarly prominent He I lines and was also classified as SNIb (Desroches et al. 2007). Another highly reddened SN candidate was detected  $2''W$ ,  $5''N$  of the galaxy nucleus on UKIRT archival K-band images taken on 1998, Dec. 5 (but not in H band, i.e.  $(H-K) > 1.2$ ; Mattila et al. 2002).

A series of spectra of SN 1999dn has been taken soon after the discovery by different groups which classified the SN as type Ia (Qiu et al. 1999b) and as type Ic because of the lack or weakness of He lines (Ayani et al. 1999; Turatto et al. 1999). Few days later the HeI lines emerged and the SN was re-classified as a SNIb/c by Pastorello et al. (1999). A week later the HeI lines strengthened again making the spectra of this SN very similar to those of other type Ib's.

Due to the early discovery, SN 1999dn was observed by several groups (Deng et al. 2000; Matheson et al. 2001).

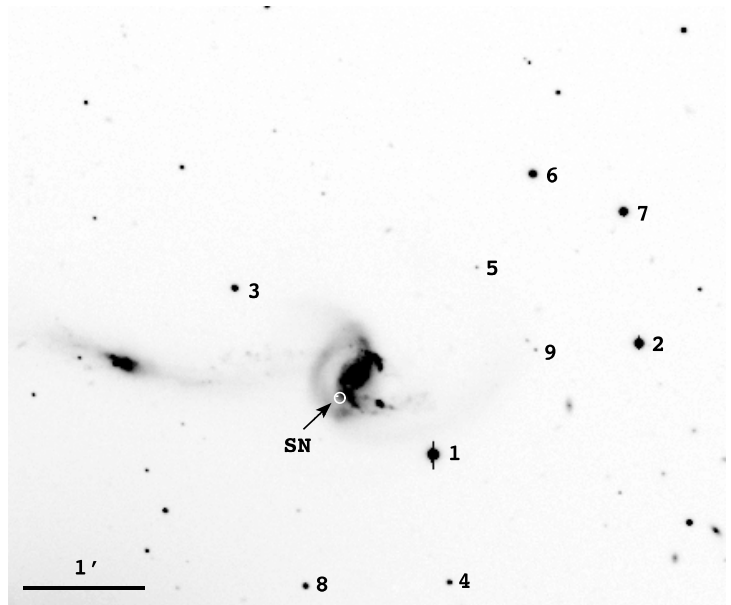


**Figure 1.** SN 1999dn in NGC 7714 and the sequence of local reference stars (cfr. Tab. 1). The image is a V frame taken with TNG+Dolores on June 28, 2000. North is up, east to the left.

It soon became one of the best-observed SNIb and a test case for extensive modeling (Deng et al. 2000; Branch et al. 2002; Ketchum, Baron, & Branch 2008; James & Baron 2010). In this paper we present original data collected at La Silla, La Palma and Asiago, and analyze them together with published material. The joint set of observations gives good multicolor photometry and dense spectral sampling, starting one week before maximum up to over two months. The SN has been recovered at late time in imaging (Van Dyk et al. 2003) and spectroscopy (Taubenberger et al. 2009).

## 2 OBSERVATIONS

UBVR<sub>I</sub>JHK' photometry of SN 1999dn was obtained at ESO-La Silla and TNG-La Palma. Ten photometric nights were used to calibrate a local sequence of stars through comparison with photometric standard stars (Landolt 1992). In turn, the local sequence was used to calibrate observations obtained during non-photometric nights. The magnitudes of the local sequence, labeled in Fig. 1, are reported in Tab. 1. The estimated errors (mean standard deviation) are reported in parentheses. Due to the small field of view of Arnica only star 1 was always included in the NIR frames, which then is the reference to check the calibration of the JHK' photometry. The averages of the measurements of this stars in three nights are reported in the footnote of Tab. 1 along with their standard deviations. The moderate dispersions of the measurements and their consistency with the 2MASS Point Source Catalogue (difference  $< 0.2mag$ ) (Skrutskie et al. 2006) add confidence to the photometric calibration.

The new photometric measurements of the SN are listed in Tab. 2. Observations were obtained on 19 different epochs up to one year after explosion. Data reduction followed standard procedures making use of a PSF fitting technique for

**Table 1.** Magnitudes of the stars of the local sequence identified in Fig. 1. The photometric errors are in parentheses (in units of  $10^{-2}$  mag).

star	U	B	V	R	I
1*	15.20(05)	14.73(03)	13.84(01)	13.43(03)	12.86(02)
2	15.76(06)	15.45(04)	14.65(02)	14.20(02)	13.80(03)
3	17.91(13)	17.35(06)	16.38(02)	15.83(01)	15.36(04)
4	19.36(16)	18.58(08)	17.62(03)	17.07(09)	16.56(06)
5	22.82:	21.57(09)	19.95(07)	18.73(03)	17.44(04)
6	16.19(02)	16.20(04)	15.44(05)	14.97(03)	14.55(06)
7	15.68(05)	15.69(03)	15.03(02)	14.64(02)	14.27(02)
8	19.83(09)	18.43(09)	17.02(04)	16.13(04)	15.47(11)
9	22.71(09)	21.31(09)	19.72(04)	18.70(05)	17.58(12)

\* J=  $12.25 \pm 0.05$ , H=  $11.50 \pm 0.10$ , K' =  $11.53 \pm 0.10$

the SN measurements. The mean photometric errors, estimated with artificial stars experiments, are given in parentheses.

The journal of the spectroscopic observations (Tab. 3) gives for each spectrum the date of observation (col.1), the phase relative to the adopted maximum (cfr. Sect. 3; col.2), the instrument (col.3), the exposure time (col.4), the wavelength range (col.5) and the resolution derived from the average FWHM of the night-sky lines (col.6). In order to improve the signal-to-noise ratio, the average of the two spectra taken on 3 and 4 September 1999 is shown in Fig. 6, after checking that there was negligible evolution. In some spectra the telluric absorptions have not been removed because of the lack of suitable standard stars with sufficient signal-to-noise ratio. In other cases, it has been impossible to remove the contamination by the underlying HII region whose lines can be either under- (e.g. day +370) or over-subtracted (day +0.8). The absolute flux calibration was verified against the B, V and R photometry. In case of disagreement, the spectra were **corrected by applying a constant factor. In fact the slit was normally aligned along the parallactic angle, in order to minimize atmospheric differential light losses (Filippenko 1982).**

### 3 PHOTOMETRY

The UBVRIJHK' light curves of SN 1999dn are shown in Fig. 2. The figure includes also the R-band data from Fig. 27 of Matheson et al. (2001) (shifted by 15.85 mag to match our observations), the late time observations of Van Dyk et al. (2003) and the pre-discovery limit by Qiu et al. (1999a). Only in the R band the light curve has been well monitored before and around maximum. A low order polynomial fit of all points around the peak provides  $JD_{max}^R = 2451420.5 \pm 0.5$  (30 Aug. 1999) at  $R_{max} = 15.85 \pm 0.05$  mag, in good agreement with the estimate by Matheson et al. (2001) (31 Aug. 1999). In the other bands the observations started a few days later and the uncertainties on the epochs of maxima are larger (cfr. Tab. 4). Following common convention we adopt the epoch of B maximum (JD 2451418.0) as reference which is 3.5 days before the reference epoch used by Matheson et al. (2001) and, later, by Branch et al. (2002), Ketchum, Baron, & Branch (2008) and James & Baron (2010).

The peak of the light curve is asymmetric with a steep

**Table 3.** Spectroscopic observations of SN 1999dn

Date	phase* (days)	inst.**	exp. (min)	range (Å)	resol. (Å)
25/08/99	-2.3	DF	45	3600-9000	9
28/08/99	+0.8	DF	45	3500-9000	9
03/09/99	+6.8	DF	45	3500-9000	9
09/09/99	+12.5	WHT	45	3200-7550	3.5
14/09/99	+17.5	EK	30	3470-7470	18
14/09/99	+17.8	EF2	15	3400-7450	14
3/11/99	+67.6	DF	120	3500-9000	10
4/11/99	+68.6	DF	120	3500-9000	10
31/08/00	+370.7	EF2	60	6000-10250	12

\*relative to the estimated epoch of B maximum (JD=2451418).

\*\*See note to Table 2 for coding, plus WHT = WHT 4.2m telescope + ISIS and EK = Asiago 1.8m telescope + AFOSC.

rise to maximum followed by a slow decline for about 10 days and a faster decrease afterwards. The contrast between maximum and inflection point as well as the width of the maximum light seems to be color dependent, with shorter wavelengths having narrower peaks and larger magnitude differences. A color dependence is visible also in the decline rate during the late radioactive tail, longer wavelengths having steeper slopes (cfr. Tab. 4). Only three epochs of NIR photometry are available: two during the early post peak decline and one in the radioactive tail. Though scanty the NIR photometry has been very useful for the construction of the bolometric flux (Sect.3.2).

A comparison of the colour evolutions of SN 1999dn with several other SN Ib/c is illustrated in Fig. 3. All objects have been dereddened according to values reported in Tab 5. An overall similarity is found among all objects of this variegated class but in the pre-maximum phase. At maximum light the B-V colors are between +0.1 to +0.6 mag and become redder afterward, reaching a maximum value (0.9 to 1.2 mag) at about 20d because of the cooling due to expansion. Thereafter the B-V colors slowly turn bluer due to the progressive increase of the emission line strengths. A good coverage before maximum is available only for the helium rich SNe 1993J, 1999ex, 2008D and 2008ax, which show very different behaviors. **Whereas the blue-band light curves of the type IIb SN 1993J showed an early peak attributed to the emergence of the shock breakout, SN 2008ax, the other SNI Ib of the sample, showed evidence of its emergence only in the very early UV light curve (Roming et al. 2009), but not in the optical (Pastorello et al. 2008; Taubenberger et al. 2010) and thus the color curve had an opposite behavior, starting red and turning bluer.** Already one week before maximum the B-V curves of both objects reach similar values (B-V= +0.15 mag) and evolve similarly afterwards. The pre-maximum difference may be attributed to the fact that SN 2008ax had a more compact progenitor and a lower density wind than SN 1993J (Chevalier & Soderberg 2010). An early peak in the blue light curves is also visible in SN 2008D and possibly in SN 1999ex. Indeed both objects show early B-V colors comparable to SN 1993J. However, the blue color peak is very short in SN 1999ex and the evolution extremely fast, with the B-V color reddening by over 1 mag in only 3 days and resembling the general trend de-

**Table 2.** Photometric measurements for SN 1999dn. The photometric errors are in parentheses (in units of  $10^{-2}$  mag).

date	JD*	U	B	V	R	I	J	H	K'	instr.
25/08/99	51415.71	16.93(06)	16.80(05)	16.18(04)	15.96(04)	15.82(06)				DF
28/08/99	51418.79	16.93(06)	16.81(05)	16.10(04)	15.80(04)	15.72(06)				DF
03/09/99	51424.77	17.23(06)	17.01(05)	16.24(04)	15.92(04)	15.65(06)				DF
06/09/99	51427.77	17.62(06)	17.15(05)	16.30(05)	15.95(06)	15.66(06)				DF
11/09/99	51433.49	18.59(06)	17.71(05)	16.59(04)	16.11(05)	15.69(05)				OIG
14/09/99	51435.76	18.71(06)	17.80(03)	16.64(03)	16.15(03)	15.81(04)				OIG
15/09/99	51436.50	18.97(09)	17.87(05)	16.76(03)	16.28(03)	15.85(03)				EF2
18/09/99	51439.77	19.28(09)	18.14(05)	16.91(03)	16.41(03)	15.95(03)				EF2
20/09/99	51441.58						15.38(15)	15.16(10)	14.92(30)	ARN
03/10/99	51455.48						15.78(10)	15.50(10)	15.31(20)	ARN
07/10/99	51459.47	19.99(09)	19.01(06)	17.81(05)	17.09(05)	16.63(05)				OIG
02/11/99	51485.35	20.14(15)	19.59(06)	18.32(06)	17.56(06)	16.88(06)				OIG
03/11/99	51485.58		19.53(05)	18.32(03)	17.57(05)					DF
04/11/99	51486.52		19.47(06)	18.30(03)	17.58(04)	16.95(05)				DF
10/12/99	51523.33	20.28(10)	19.89(08)	18.82(07)	18.02(07)	17.30(07)				OIG
27/12/99	51540.32		19.94(08)	19.11(07)	18.20(07)	17.59(07)				OIG
27/12/99	51540.37						17.93(20)	17.46(25)	17.64(30)	ARN
28/06/00	51723.69			22.57(35)	20.78(20)					Dol
31/08/00	51788.60			$\geq 23.15(70)$	21.93(50)					EF2

\* 2400000+

DF = ESO/Danish 1.5m telescope + DFOSC

OIG = Telescopio Nazionale Galileo + OIG CCD Camera

EF2 = ESO 3.6m telescope + EFOSC2

ARN = Telescopio Nazionale Galileo + ARNICA IR Camera

Dol = Telescopio Nazionale Galileo + Dolores

scribed for SN 2008ax thereafter. The behavior of SN 1999ex leaves room for the presence of early, short shock breakout signatures also in other objects.

The colors of SN 1999dn are available only from around maximum, but the spectral evolution in the week before (cfr. Sect. 4) indicates **that the SED has become bluer and bluer from day -6 to maximin light, which suggests a color evolution for SN 1999dn more similar to SNe 1999ex and 2008ax than to SN 1993J**. After reaching a maximum value of B-V similar to all other SNIb/c, SN 1999dn remained unusually red up to over 100 days. The adoption of an higher extinction correction might reduce the difference (cfr. Sect. 3.1).

The R-I color evolutions of SE-SNe are smoother and remain confined between -0.3 mag at maximum and +0.7 mag later on. All objects show similar evolution and SN 1999dn is in the troop. The outlier here is SN 1993J, which remains bluer at all epochs.

### 3.1 Reddening and absolute magnitudes

The interstellar NaID lines arising both from our and the parent galaxy are well seen in the low-resolution spectra at about 5893 and 5945 Å, respectively. Therefore the reddening of SN 1999dn cannot be neglected. Schlegel et al. (1998) give a galactic reddening  $E_{MW}(B-V) = 0.052$  mag in the direction to NGC 7714. We have measured the EWs of the NaID components in the spectra of SN 1999dn on the spectrum of highest signal-to-noise and resolution (WHT on 9 Sept., res. 3.5 Å) and found an  $EW_{MW}(\text{NaID}) \sim 0.51$  Å and  $EW_{N7714}(\text{NaID}) \sim 0.45$  Å. These values are in good agreement with the average of EW measurements performed on

**Table 4.** Main data of SN 1999dn

position (2000.0) <sup>a</sup>	23 <sup>h</sup> 36 <sup>m</sup> 14.81 <sup>s</sup>		+02°09′m08 <sup>s</sup> .4	
parent galaxy	NGC 7714, SBb pec <sup>b</sup> with starburst <sup>c</sup>			
offset wrt nucleus	9.9″E		9.4″S	
adopted distance modulus	μ = 32.95 ± 0.11			
SN heliocentric velocity	2630 ± 150 km s <sup>−1</sup>			
adopted reddening	E <sub>MW</sub> (B−V) = 0.052 <sup>d</sup>		E <sub>tot</sub> (B−V) = 0.10 ± 0.05	
<hr/>				
	peak time (JD−2451000)	peak observed magnitude	peak absolute magnitude	
U	418 ± 2	16.9 ± 0.1	−16.6 ± 0.5	
B	418 ± 2	16.8 ± 0.1	−16.6 ± 0.4	
V	419 ± 1	16.1 ± 0.1	−17.2 ± 0.4	
R	420.5 ± 0.5 <sup>e</sup>	15.85 ± 0.05	−17.35 ± 0.40	
I	424 ± 1	15.60 ± 0.05	−17.55 ± 0.35	
uvoir	419.5 ± 0.5		L <sub>bol</sub> = 2.0 × 10 <sup>42</sup> erg s <sup>−1</sup>	
rise to max	~ 12 days			
explosion day	~ 406	~ 16 Aug. 1999		
<hr/>				
	late time decline mag (100d) <sup>−1</sup>	interval days	late time decline mag (100d) <sup>−1</sup>	interval days
U	0.37	67–105		
B	0.81	67–122		
V	1.79	67–306	1.43	67–122
R	1.44	67–370	1.17	67–122 <sup>f</sup>
I	1.64	67–515	1.19	67–122
uvoir	1.49	67–122		
<hr/>				
M( <sup>56</sup> Ni)	0.11 M <sub>⊙</sub>			
M(ejecta)	4–6 M <sub>⊙</sub>			
explosion energy	5.0–7.5 × 10 <sup>51</sup> erg			

a- Qiu et al. (1999a), b- <http://leda.univ-lyon1.fr>, c- Weedman et al. (1981), d- Schlegel et al. (1998), e- 30 Aug. 1999, f- our data only

all other available spectra with no evidence of significant time evolution. Assuming that the gas/dust properties in NGC 7714 and the Galaxy are the same, we estimate a

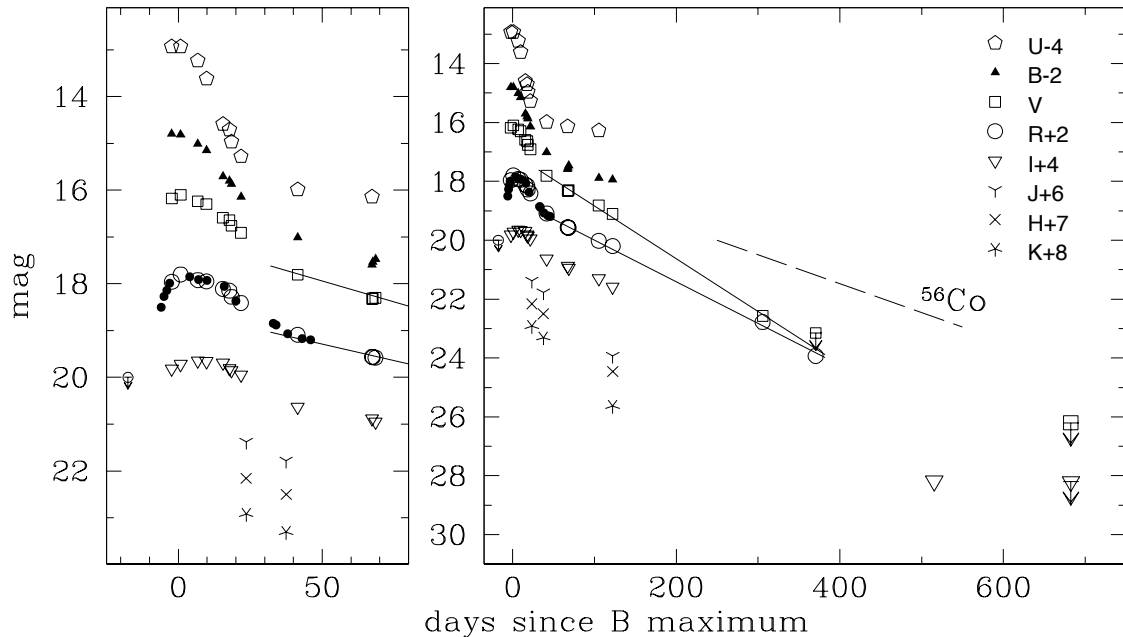


**Figure 2.** UBVRIJHK' light curves of SN 1999dn. The left panel is a zoom around the epoch of maximum, while the whole evolution is shown in the right panel. The R band observations by Matheson et al. (2001) are reported as small filled circles, shifted to match our R magnitudes. The predisccovery unfiltered limit by Qiu et al. (1999a) is reported in the R band scale (open circle + arrow). Late time ( $> 500$ d) F550W and F814W observations by Van Dyk et al. (2003) are reported in the V and I scale, respectively, as large symbols. To guide the eye, the late time V and R observations have been fitted by straight lines, while a dashed line is drawn to show the slope of  $^{56}\text{Co}$  decay.

total reddening  $E_{\text{tot}}(B - V) = 0.098$  mag. A similar value  $E_{\text{tot}}(B - V) = 0.131$  mag is obtained by using the average relation between  $E(B - V)$  and  $\text{EW}(\text{NaID})$  (Turatto, Benetti, & Cappellaro 2003). Finally, the match of the color curves of SN 1999dn to those other SE SNe (cfr. Sect. 3) suggests a consistent, though formally slightly higher reddening,  $E(B - V) \sim 0.15$ . Throughout this paper we adopt for SN 1999dn a total reddening  $E_{\text{tot}}(B - V) = 0.10 \pm 0.05$  mag ( $A_V = 0.31$  mag).

Since there is no direct measurements of the distance to NGC 7714, we use the Hubble's law. From the wavelength of the interstellar NaID absorption features we derive a recession velocity of  $2630 \pm 150$   $\text{km s}^{-1}$ , which is consistent with the heliocentric radial velocity reported by LEDA<sup>1</sup> ( $2797 \pm 16$   $\text{km s}^{-1}$ ). LEDA provides also a velocity corrected for the Local Group infall into the Virgo cluster  $v_{\text{Vir}} = 2798$   $\text{km s}^{-1}$ . Adopting  $H_0 = 72$   $\text{km s}^{-1} \text{Mpc}^{-1}$ , we derive a dis-

tance modulus  $\mu = 32.95$  mag which is used throughout this paper<sup>2</sup>.

Adopting the above mentioned values for extinction and distance, we obtain the following absolute magnitudes at maximum  $M_U = -16.6 \pm 0.5$ ,  $M_B = -16.6 \pm 0.4$ ,  $M_V = -17.2 \pm 0.4$ ,  $M_R = -17.35 \pm 0.40$  and  $M_I = -17.55 \pm 0.35$ , where in the computation of the errors we adopted an uncertainty of  $\pm 250$   $\text{km s}^{-1}$  on the Hubble distance modulus due to possible peculiar motion.

**We note that, after rescaling to a common distance scale, our determination of  $M_V$  is 0.5 mag brighter than that derived by Richardson, Branch, & Baron (2006), but in good agreement with the mean value of  $M_R = -17.01 \pm 0.41$  given by Li et al. (2010) for a sample of six SNIb, SN 1999dn included. In comparison to the subsamples studied in Li et**

<sup>2</sup> A similar value ( $\mu = 32.84$ ) is obtained adopting the distance relative to the Virgo cluster in the 220 model (Kraan-Korteweg 1995) with  $D(\text{Virgo}) = 15.3$  Mpc (Freedman et al. 2001).

<sup>1</sup> <http://leda.univ-lyon1.fr>

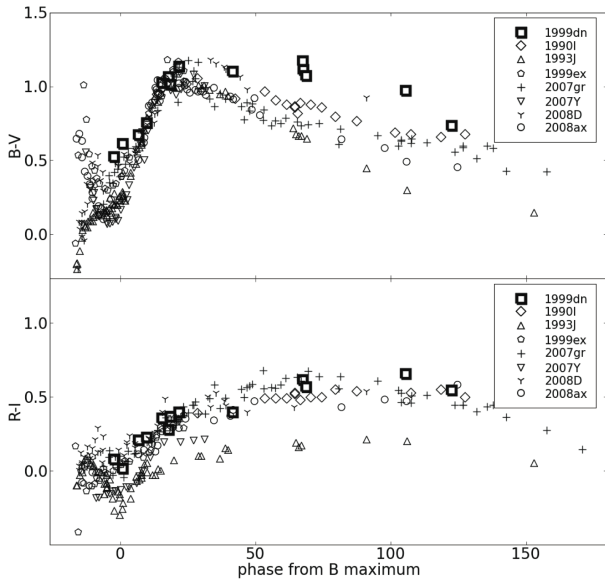


**Figure 3.** Top panel: Comparison of the B–V color curve of SN 1999dn with those of other SE–SNe. The curves have been dereddened with the values reported in Tab. 5 and a standard extinction law. Bottom panel: as above, but for the observed R–I color curve (r–i for SN 2007Y).

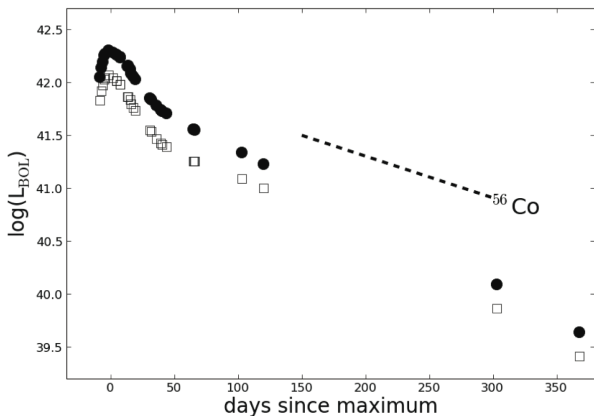


**Figure 4.** UBVRJHK' bolometric (filled circles) and UBVR (open squares) light curves of SN 1999dn. The points on the rising branch and those after 4 months past maximum are largely based on extrapolations (assuming constant colors) and should be regarded as uncertain. The slope of  $^{56}\text{Co}$  to  $^{56}\text{Fe}$  decay is also displayed for comparison.

al., SN 1999dn remains about 0.80 mag brighter than their unweighted mean for the *normal* SE SNe (SNIc+Ib+IIb).

### 3.2 Bolometric light curve

With the available photometry it has been possible to build the UBVRJHK' bolometric light curve up to 1yr (Fig. 4).

When magnitudes in a bandpass were not available in a given night, the values were linearly interpolated. The light curves with a short temporal extension, e.g. those in the NIR, were extrapolated assuming constant colors. For this reason the bolometric flux during the rising branch and those at the latest epochs are based mainly on R band observations and should be regarded as uncertain. The photometry was corrected for extinction using  $R_V = 3.1$ . At the effective wavelengths of each filter monochromatic fluxes were computed; these were then integrated from the U to K' bands using the trapezoid approximation, and converted to luminosity. The peak of the bolometric light curve is reached between the V and the R maxima on  $\text{JD}_{\text{max}}^{\text{bol}} = 2451419.5 \pm 0.5$  at a luminosity  $L_{\text{bol}} = 2.0 \times 10^{42} \text{ erg s}^{-1}$ .

The contribution of the NIR bands is substantial at all the epochs in which NIR data are available ( $L_{\text{JHK}}/L_{\text{uvoir}} = 0.5, 0.5$  and  $0.4$  at day 20, 40 and 121, respectively). This is more than a factor two larger than the value derived for SNIb 2007Y (Stritzinger et al. 2009) and for SN 2008D (Modjaz et al. 2009), but similar to values derived for SNIb 2008ax (Taubenberger et al. 2010). In the photospheric phase, the optical+NIR SED deduced from SN 1999dn photometry is consistent with a blackbody energy distribution with temperatures as derived from optical spectra (cfr. Sect. 4). The decline rate between 67d and 122d is  $1.49 \text{ mag (100d)}^{-1}$ , close to the average value of type Ia SNe. This value is significantly larger than the decline rate of  $0.98 \text{ mag (100d)}^{-1}$  predicted if all the energy from the decay of  $^{56}\text{Co}$  into  $^{56}\text{Fe}$  was fully thermalized. No significant slope variation is observed up to day 370 ( $\gamma_{\text{uvoir}} = 1.65 [67\text{d}-305\text{d}]$ ).

In Fig. 5 we compare the bolometric light curve of SN 1999dn with those of other SE SNe. Unfortunately not all have coverage from optical to NIR wavelengths. The comparison has been done both for the extended *uvoir* (UBVRJHK', top panel) and the optical-only (UBVR, bottom panel) bolometric curves.

The rise to maximum can be very different. The type IIb SN 1993J shows an early bright spike about 20d before a broader secondary maximum. For the other SNIb caught early-on, SN 1999ex (bottom panel), the bolometric light curve shows just an hint of the shock breakout.

For the peculiar SN 2005bf a slow rise to a first maximum is observed followed about 25d later by a second brighter maximum. The type Ib SN 2007Y and the type Ic SNe 1994I, 2004aw and 2007gr were not detected sufficiently early after the explosion and do not show any feature in the rising branch. The first reliable photometry of SN 1999dn has been obtained 6 days before B maximum (8.5d before R maximum), while the available pre-discovery limit does not put stringent constraints on the date of explosion. The direct comparison with other SNIb/c suggests a rise time (**relative to B maximum**) similar to SN 2007gr, i.e.  $11.5 \pm 2.0$  days (Hunter et al. 2009).

The contribution of the JHK' bands to the bolometric flux of SN 1999dn stands out: while in the UBVR domain it has almost the same luminosity as the type Ic SN 2007gr, in the *uvoir* it outpaces it by about 0.12 dex.

The asymmetric peak of SN 1999dn, with a relatively fast rise and slow decline, reminds of the behavior of SN 2007gr, but with even slower decline. After maximum the bolometric light curve remains relatively broad and closely resembles in

**Table 5.** SE SNe used for color and bolometric luminosity comparison.

SN	Host Galaxy	SN type	$E_{tot}(B-V)$	(m-M)	main references
1999dn	NGC 7714	Ib	0.10	32.95	Sect. 3.1 of this paper
1990I	NGC 4650A	Ib	0.16	32.90	Elmhamdi et al. (2004)
1993J	NGC 3031	IIb	0.30	27.80	Barbon et al. (1995); Richmond et al. (1996b)
1994I	NGC 5194	Ic	0.45	29.75	Richmond et al. (1996a); Dessart et al. (2008)
1999ex	IC 5179	Ib	0.28	33.19	Stritzinger et al. (2002)
2004aw	NGC 3997	Ic	0.37	34.17	Taubenberger et al. (2006)
2005bf	MCG +00-27-5	Ib/c	0.05	34.46	Folatelli et al. (2006)
2007Y	NGC 1187	Ib	0.11	31.13	LEDA, Stritzinger et al. (2009)
2007gr	NGC 1058	Ic	0.09	29.84	Valenti et al. (2008a); Hunter et al. (2009)
2008D	NGC 2770	Ib	0.66	32.29	Mazzali et al. (2008); Modjaz et al. (2009)
2008ax	NGC 4490	IIb	0.40	29.92	Pastorello et al. (2008); Taubenberger et al. (2010)

shape that of SN 2004aw, but remains about 0.3 dex fainter at all epochs. This simple comparison indicates that adopting the Arnett model (Arnett 1982) at the early times, when the diffusion approximation is valid, the amount of  $^{56}\text{Ni}$  synthesized in the explosion of SN 1999dn is between 0.10 and 0.15  $M_{\odot}$  ( $M_{Ni}(2007gr)=0.076 M_{\odot}$ , Hunter et al. (2009);  $M_{Ni}(2004aw)=0.30 M_{\odot}$ , Taubenberger et al. (2006)). Broad light curves are indicative of large diffusion time and hence of either a large ejected mass or a small kinetic energy. The comparison of the expansion velocity of SN 1999dn (cfr. Sec. 4.1) with other SE SNe suggests that the long diffusion time is due to a large ejecta mass of SN 1999dn, much larger than that of the narrow-peak SN 1994I (cfr. Fig. 5). A more detailed discussion of the explosion parameters is given in Sect. 5.

#### 4 SPECTROSCOPY

The entire spectroscopic evolution of SN 1999dn from about 1 week before maximum to over 1 yr is illustrated in Fig. 6, thanks to the spectra listed in Tab. 3 and those published by Deng et al. (2000) and Matheson et al. (2001). The SN evolution is therefore well sampled at all crucial phases. We stress again that the phases adopted here, are relative to the date of B maximum (JD 2451418.0) and differ from those used in previous papers (cfr. Sect. 3).

The **first spectrum** (−6d, Aug.21) has been subject to deep scrutiny. Deng et al. (2000) have modeled it with SYNOW using a black-body temperature  $T_{bb}=7500$  K and photospheric velocity  $v_{ph}=16000 \text{ km s}^{-1}$ . Besides the broad absorptions at 4750 and 4950 Å (restframe) due to FeII, and at about 8200 Å due to CaII IR, the spectrum is dominated by the HeI  $\lambda 5876$  and  $\lambda 7065$  which contribute to the strong 5620 Å and 6820 Å features. The broad absorption at about 6200 Å has attracted the attention of Deng et al. and other modelers and will be extensively discussed in Sect. 4.1. This spectrum has been modeled also by Branch et al. (2002) who used SYNOW with line optical depths varying as  $v^{-n}$  and  $n = 8$  instead of  $e^{-v/v_e}$  ( $v_e = 1000 \text{ km s}^{-1}$ ) as in Deng et al. (2000). The spectrum was well reproduced with slightly lower temperature and velocity ( $T_{bb}=6500$  K and  $v_{ph}=14000 \text{ km s}^{-1}$ ) and the same contributing ions. Ketchum, Baron, & Branch (2008) modeled this and the other spectra around maximum with their non-LTE code

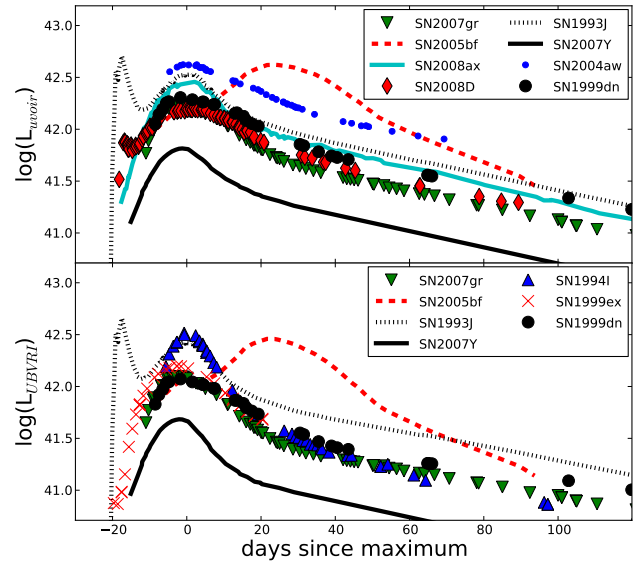


**Figure 5.** Comparison of the bolometric light curve of SN 1999dn with those of other type Ib/c SNe. **The phase is from B maximum.** The comparison based on the whole optical-NIR (uvoir) domain is in the top panel, that based on the UVBRI bands (uBgVri for SN 2005bf, UuBgVri for SN 2007Y) in the bottom panel. The SN distances and reddening are reported in Tab. 5. Note that with the adopted distance and reddening SN 1994I is among the brightest objects. Small misalignments in the epochs of maxima are due to different choices of the reference epochs.

PHOENIX trying both a standard solar and a three times higher metallicity. Although they adopted a smaller extinction ( $E(B-V)=0.052$  mag) and later explosion epoch (12 days before Aug.31) with respect to the values that we now consider more realistic (cfr. Tab. 4), their fit is good also for the non-thermal HeI lines. The other features were identified with CaII, FeII and OI. Similar results were obtained also by James & Baron (2010) who, as it appears, did not correct for extinction. Their model parameters ( $T_{mod}=6000$  K and  $v_0 = 11000 \text{ km s}^{-1}$ ) are slightly smaller than the values



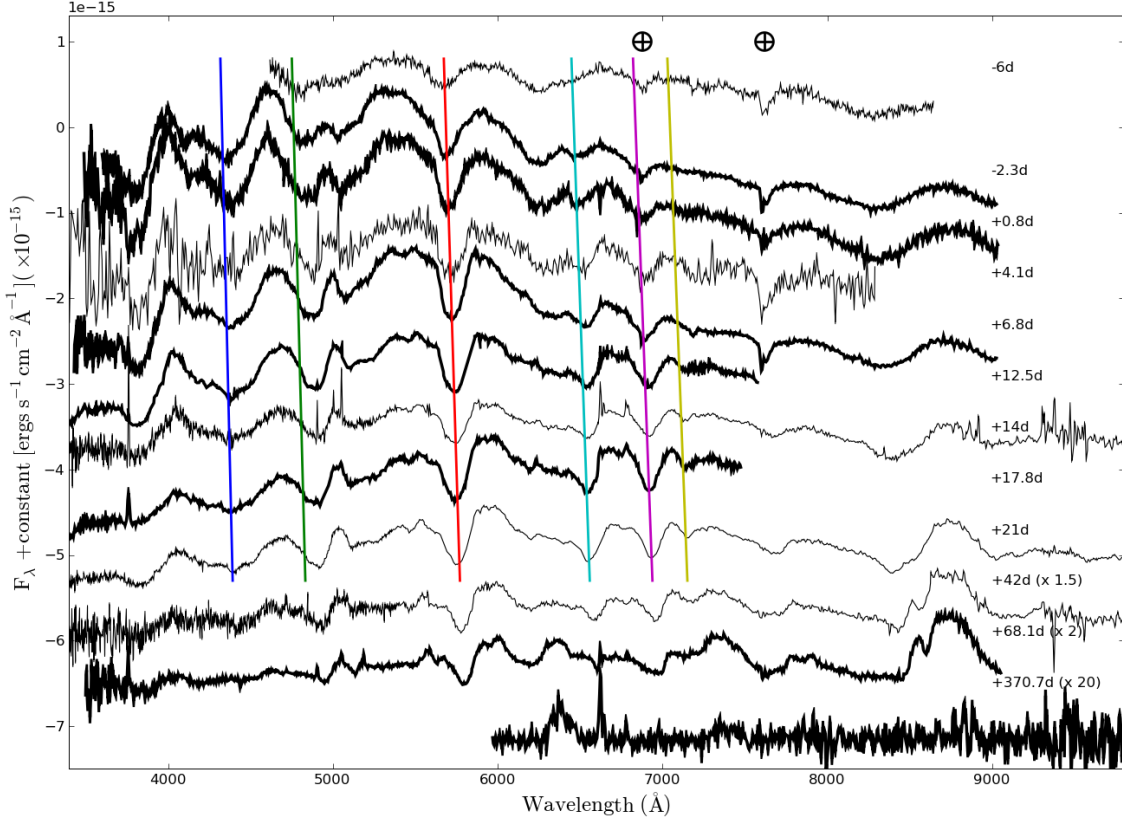


**Figure 6.** The overall spectral evolution of SN 1999dn (including spectra by Deng et al. 2000 and Matheson et al. 2001 as thin lines). The wavelength is in the observer rest frame and the flux is not corrected for reddening. The ordinate refers to the top spectrum; other spectra are shifted downwards with respect to the previous by  $1.2 \times 10^{-15}$  (second spectrum) and  $0.6 \times 10^{-15} \text{ erg s}^{-1} \text{ cm}^{-2} \text{ Å}^{-1}$  (others). The spectra taken on Nov. 3 and 4 have been averaged, while for Sept. 14 only the EFOSC2 spectrum is displayed. Vertical lines correspond to the positions of HeI  $\lambda 4472$ ,  $\lambda 4921$ ,  $\lambda 5876$ ,  $\lambda 6678$ ,  $\lambda 7065$  and  $\lambda 7281$ , with expansion velocities of  $13000 \text{ km s}^{-1}$  at the earliest epoch and then slowing down with time. Each spectrum is labelled with the phase with respect to the B maximum (JD=2451418.0). For clarity the last three spectra have been multiplied by the factors reported in parentheses. Telluric features are marked with the Earth symbol.

( $T_{\text{bb}} = 6700 \pm 200 \text{ K}$  and  $v_{\text{ph}} = 12800 \text{ km s}^{-1}$ ) we derive by fitting the de-reddened spectrum<sup>3</sup>.

Our new observations provide a good coverage of the epoch of maximum with spectra on **days -2.3 and +0.8**. At this phase the object has become bluer and hotter, reaching  $T_{\text{bb}} = 9100$  and  $7800 \text{ K}$ , respectively. The line contrast is now higher with more pronounced absorption troughs and broad emissions. The HeI lines have become stronger so that the  $\lambda 6678$  line is clearly identified in addition to the  $\lambda 5876$  and  $\lambda 7065$  lines. In the blue strong H & K CaII and FeII lines are visible which indicate photospheric expansion velocities  $v_{\text{ph}} = 10400$  and  $10000 \text{ km s}^{-1}$ , respectively.

The next available spectrum on **day +4.1, Aug. 31**, though quite noisy, has been modeled using both SYNOW ( $T_{\text{bb}} = 7000 \text{ K}$  and  $v_{\text{ph}} = 12000 \text{ km s}^{-1}$ , Deng et al. 2000;  $v_{\text{ph}} = 10000 \text{ km s}^{-1}$ , Branch et al. 2002) and PHOENIX

(Ketchum, Baron, & Branch 2008) giving an effective temperature of  $6000\text{--}6500 \text{ K}$  and  $v_{\text{ph}} = 10000 \text{ km s}^{-1}$ . The features are well fit by the same ions as on day -6 (CaII, FeII, HeI and OI). The model with standard solar metallicity reproduces fairly well also the He lines both in absorption and in emission. Again the best fit temperature by James & Baron (2010) is lower ( $T_{\text{mod}} = 5250 \text{ K}$ ). Our black-body fit to the dereddened spectrum of day +4.1 provides  $T_{\text{bb}} \sim 6400 \text{ K}$  which is lower than the values derived for the two bracketing epochs ( $T_{\text{bb}} = 7800$  and  $7000 \text{ K}$  for day +0.8 and 6.8, respectively) possibly because of a poor instrument response calibration. The position of the Fe lines at about  $5000 \text{ Å}$  corresponds to  $v_{\text{ph}} = 10000 \text{ km s}^{-1}$ , in good agreement with the velocities derived in the spectral modeling.

Of much better quality ( $S/N > 100$ ) is the spectrum obtained on **day +6.8**. The fit to the SED provides  $T_{\text{bb}} = 7000 \text{ K}$ , and the expansion velocity from the FeII lines decreases to  $v_{\text{ph}} = 8600 \text{ km s}^{-1}$ .

In the following week the evolution slows down. Two spectra are available on **day +12.5 and +14**, the former with an excellent signal-to-noise ( $S/N = 150$ ) and resolu-

<sup>3</sup> Note that de-reddening the spectra as in Sect. 3.1 the temperatures of the SN 1999dn spectra increases on average by 6–8 %.



tion (3.5 Å), the latter with wider spectral range (Matheson et al. 2001). Our analysis provides a similar temperature,  $T_{\text{bb}} \sim 5500$  K in both spectra, but significantly different photospheric velocities ( $v_{\text{ph}} = 6400$  and  $4900$  km s $^{-1}$ , respectively). Both the Galactic NaID lines as well as those originating in the host galaxy are well resolved, as mentioned in Sect. 3.1. HeI  $\lambda 5876$  is very broad and possibly heavily contaminated by NaID. Also the lines at  $\lambda 6678$  and  $\lambda 7065$  clearly stand out, whereas others ( $\lambda 4472$  and  $\lambda 7281$ ) are less pronounced (the former probably blended with MgII). The well developed HeI lines make the spectrum closely resemble that of prototypical Type Ib supernovae. Ketchum, Baron, & Branch (2008) have studied the spectrum of day +14: again the solar metallicity model fits the observations better, though the CaII and HeI absorptions are too strong. TiII starts to contribute significantly to the FeII dominated region below 5000 Å.

Three spectra have been obtained on Sept. 14 (**day +17.5 to +17.8**) at different telescopes (cfr. Tab. 3 and Deng et al. 2000). The SEDs of our two spectra are similar ( $T_{\text{bb}} = 4800$  K) but the S/N ratio of that obtained with EFOSC2 (plotted in Fig. 6) is definitely higher. The Deng et al. (2000) spectrum, significantly bluer ( $T_{\text{bb}} = 5700$  K), has been used in the modeling both by Deng et al. (2000) and Ketchum, Baron, & Branch (2008). Again the standard composition model seems to be preferred though with too strong HeI and CaII absorptions. The index  $n$  of the density profile  $\rho \propto r^{-n}$  was decreased from 13 to 10 to improve the fit.

The subsequent spectra (**day +21 and +42**, i.e. Sept. 17 and Oct. 8) come from Matheson et al. (2001). At both epochs the main features and the SEDs have not changed significantly with respect to day +18. We measure  $T_{\text{bb}} \sim 4900$  K on the dereddened spectrum, in good agreement with the temperature adopted in the modeling (respectively 4800 and 4600 K, Branch et al. 2002; James & Baron 2010). The measured expansion velocities are  $v_{\text{ph}} = 5500$  and  $4600$  km s $^{-1}$ , respectively. In the latter spectrum one can notice that the CaIR triplet starts to be resolved with an absorption at about 8360 Å, corresponding to a velocity  $v(\text{CaII}) \sim 7700$  km s $^{-1}$ . As the temperature of the SN has decreased to about 5500 K, the region bluer than 5000 Å is largely dominated by TiII lines (Ketchum, Baron, & Branch 2008). This explains why the high metallicity model fails to reproduce the observations causing too strong absorptions.

The latest spectrum of the photospheric series (**day +68**) is the average of two spectra taken with the same instrument on two consecutive nights. The HeI lines are still visible as well as the underlying continuum ( $T_{\text{bb}} = 4400$  K). Nevertheless, the progressive transition to the nebular phase can be recognized. In particular, the broad [OI]  $\lambda\lambda 6300, 6364$  and [CaII]  $\lambda\lambda 7291-7323$  ([OII]  $\lambda\lambda 7320, 7330$ ) features start to appear clearly.

The characterizing features of the nebular spectra of SNIb/c are, indeed, [OI] and [CaII] emission lines. These are well developed at the epoch of our last spectroscopic observation (**day 371**). Once deblended into its two components, the [OI] line has an overall gaussian profile centered slightly redward of the restframe position (6309 Å) with FWHM  $\sim 4500$  km s $^{-1}$ , though the relatively poor signal-to-noise ratio still allows for the presence of additional structures in the line profile (Taubenberger et al. 2009). In any

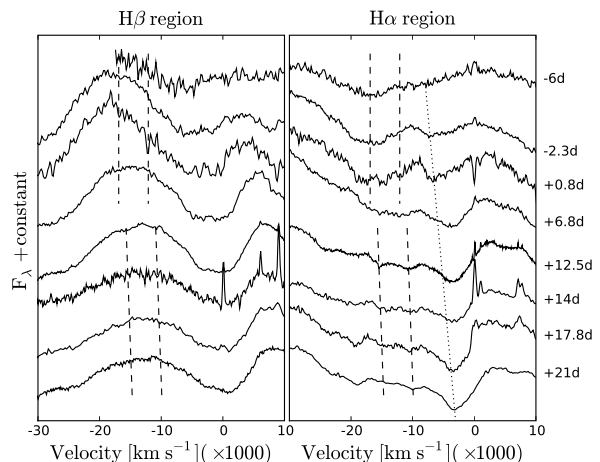


**Figure 7.** Zoom of the 4600 Å (left) and 6200 Å (right panel) spectral regions during the first weeks of evolution of SN 1999dn. The x axes are in expansion velocity coordinates with respect to the rest frame positions of H $\beta$  and H $\alpha$ , respectively. The phases relative to B maximum light are indicated on the right axis. To guide the eye two dashed vertical lines are drawn in the spectra around maximum, corresponding to expansion velocities of about 16900 and 12100 km s $^{-1}$ . After day +12.5 the broad 6200 Å feature is replaced by two narrower and weaker features which slightly slow down with time. Corresponding lines are drawn also in the left panel relative to H $\beta$ . The dotted line in the right panel is drawn at the position of HeI  $\lambda 6678$ .

case there is no evidence for profile distortion or a blueshift due to dust formation as detected in other objects (e.g. SN 1990I, Elmhamdi et al. 2004) in the same [OI] line.

#### 4.1 The expansion velocities and the presence of Hydrogen

Hydrogen lines at early epochs distinguish the spectra of SNIb from other SE SNe. Actually, faint H lines have been revealed unambiguously in the type Ib SN 2000H and, with lower confidence, in other SNIb (Branch et al. 2002; James & Baron 2010). These authors concluded that H is present with low optical depths in SNIb in general and that it is located in a detached shell with velocities as high as 11000–13000 km s $^{-1}$ . In this context, some attention has been paid in the previous spectral analyses of SN 1999dn (Deng et al. 2000; Branch et al. 2002; Ketchum, Baron, & Branch 2008; James & Baron 2010) to a broad feature present in the spectra around maximum at about 6200 Å.

The feature seen in the first epoch (day -6) was attributed by Deng et al. (2000) to H $\alpha$  or CII  $\lambda 6580$ , arising in a detached layer with velocity  $v = 19000$  or  $20000$  km s $^{-1}$ , respectively. Also Branch et al. (2002) interpreted the feature as due to H $\alpha$  from a detached layer of H at 18000 km s $^{-1}$ . The possible alternative identification as SiII, proposed by Woosley & Eastman (1997) for SN 1984L, results in an expansion velocity (7300 km s $^{-1}$ ) significantly lower than that of any other ion and is, therefore, considered unlikely. Similar identifications were proposed for the spectra of day +4.1 (H $\alpha$ , Branch et al. 2002, possibly blended with CII, Deng et al. 2000) and day +17 and +21 (CII, Deng et al. 2000, or FeII, Branch et al. 2002). The spectra were revisited by

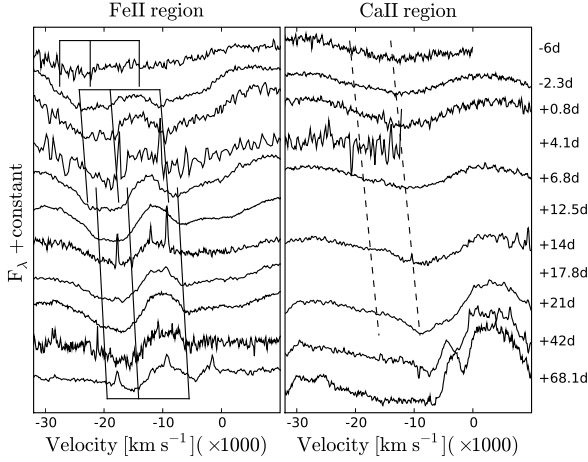


**Figure 8.** Zoom of the FeII (left) and CaII IR (right panel) spectral regions during the first months of evolution of SN 1999dn. In the left panel, the approximate positions of FeII  $\lambda 4924$ ,  $\lambda 5018$  and  $\lambda 5169$  are marked. The velocity reported on the abscissa refers to the  $\lambda 5169$  line and ranges from  $-14000$  to  $-5500 \text{ km s}^{-1}$  from day  $-6$  to day  $68$  past B maximum. In the right panel two dashed lines are drawn to guide the eye for the main component (right) and the possible high velocity feature (left) of CaII.

Ketchum, Baron, & Branch (2008). They found that at early times, when the  $6200 \text{ \AA}$  feature is strong and broad, an uniform atmosphere of three times solar metallicity, devoid of any H, could provide a plausible explanation, making the feature a blend of FeII lines and SiII  $\lambda 6355$ . At later times the feature splits into multiple, distinct, weaker features, and solar metallicity fits better. However, they admit that higher metallicity in the outer envelope (as seen in the early time spectra) is difficult to explain, **also in the light of our direct determination of a somewhat sub-solar metallicity for the SN environment (c.f.r. Sect 5)**. The simpler interpretation of the  $6200 \text{ \AA}$  feature, therefore, seems to be the presence of H. The new, specific analysis by James & Baron (2010) confirms this identification and suggests a H mass of  $M_H \leq 10^{-3} M_\odot$  in an outer shell of solar composition above the He core.

With this work we add new, high signal-to-noise spectra around maximum, and readdress the issue of the possible presence of H. In Fig. 7 we have zoomed into the H $\alpha$  (right panel) and H $\beta$  (left panel) regions of the best available spectra. To guide the eye in the right panel we have drawn two vertical dashed lines corresponding to velocities of  $-16900$  and  $-12100 \text{ km s}^{-1}$  at the earliest epoch, assuming the H $\alpha$  identification. The dotted line at lower velocity indicates the position of HeI  $\lambda 6678$  (the same as in Fig. 6). The line is tilted to roughly match the velocity decrement. Contrary to HeI, the  $6200 \text{ \AA}$  feature appears at constant velocity ( $-16900 \text{ km s}^{-1}$ ) up to maximum light, while a notch at about  $-12000 \text{ km s}^{-1}$  might be present. Should these features be due to single lines and not to the conspiring effect of line blending (e.g. FeII and SiII), the constancy in expansion velocity is an indication of detached layers. Note that the blue wing of the strong HeI  $\lambda 5876$  line extends outward to about  $-18000 \text{ km s}^{-1}$  on day  $-6$  and  $-15500 \text{ km s}^{-1}$  on day  $+0.8$ , close to the estimated velocity of the fastest H layer.

By day  $+6.8$  the broad  $6200 \text{ \AA}$  feature has disappeared. Starting on day  $+12.5$  down to day  $+21$  two distinct, resolved features spaced by about the same amount as before are clearly visible. They were noted by Ketchum, Baron, & Branch (2008) who suggested the same possible interpretation with FeII, SiII, CII and TiII. The slower component, if identified with H $\alpha$ , shows marginally higher velocity than HeI  $\lambda 6678$  and slows down with time at the same rate ( $\sim 1000 \text{ km s}^{-1}$  in  $10\text{d}$ ).

To check whether this pair of lines are due to H, we have drawn two lines at corresponding velocities on the left panel of Fig. 7 relative to H $\beta$ . Although the H $\beta$  optical depth is expected to be significantly smaller than that of H $\alpha$ , we note that possible signatures of H $\beta$  are recognizable at the expected positions in the spectra of days  $-2.3$  and  $+12.5$ , the latter having the best signal-to-noise and spectral resolution. Though not compelling, we consider this an additional evidence that H is present in the spectrum of SN 1999dn both in a detached layer above the photosphere and mixed with HeI.

A  $6250 \text{ \AA}$  feature was identified as H $\alpha$  in the early spectra of the peculiar SN 2005bf at comparable velocity ( $\sim -15000 \text{ km s}^{-1}$ ) on the basis of the detection of similar tiny features at the corresponding position of H $\beta$  (Folatelli et al. 2006). Also CaII and FeII lines had components with similar expansion velocity. For this reason we have investigated the possible presence of high velocity features for both these ions also in SN 1999dn. In Figure 8 the spectral regions of interest are plotted in analogy to those in Fig. 7. Broad and shallow FeII lines seem present early on also in SN 1999dn at about  $-14000 \text{ km s}^{-1}$ , a velocity exceeding that measured for HeI ( $-12700 \text{ km s}^{-1}$ ) and expected for the photosphere on day  $-6$ . The FeII lines are easily detected at smaller velocity in the following spectra. Strong, broad CaII IR triplet absorption is detected at a velocity comparable to that of HeI. In the spectra of highest signal-to-noise ratio (day  $+6.8$  and  $+14$ ) one may also see another component about  $5000 \text{ km s}^{-1}$  faster but the first detection of high velocity features of CaII starting at this epoch makes the identification unlikely. We conclude that, in addition to H $\alpha$ , there is evidence of weak high-velocity FeII features before maximum.

In Fig. 9 (top panel) we summarize the evolution of the line velocities as a function of time. The standard deviation of the velocities derived for HeI lines is  $\sigma = 400 - 700 \text{ km s}^{-1}$ , possibly due to blending of various lines (e.g. NaID for  $\lambda 5876$ , contamination by telluric features for  $\lambda 7065$ , or by narrow H $\alpha$  emission of the parent galaxy for  $\lambda 6678$ ). We estimate uncertainties of the same order for the possible H lines because of their weakness. The photospheric velocity of SN 1999dn is in agreement with those of other normal SNIb (Branch et al. 2002) and is well fitted by the power-law,  $v_{ph} \propto t^{-2/(n-1)}$  with  $n = 3.6$ . As for other SNIb, HeI seems to be undetached at the first epoch but detached afterward. The lowest velocity of the HeI layer is measured at about  $6000 \text{ km s}^{-1}$ . The faster H is detached at all epochs with velocity ranging between  $17000 - 13000 \text{ km s}^{-1}$ . The slower H component remains about  $1500 \text{ km s}^{-1}$  faster than HeI at all epochs. The two H components somehow bracket the H velocities of other SNIb reported in Fig. 23 of Branch et al. (2002).

The bottom panel of Fig. 9 compares the FeII velocity of SN 1999dn with those of other SE SNe. SN 1999dn has

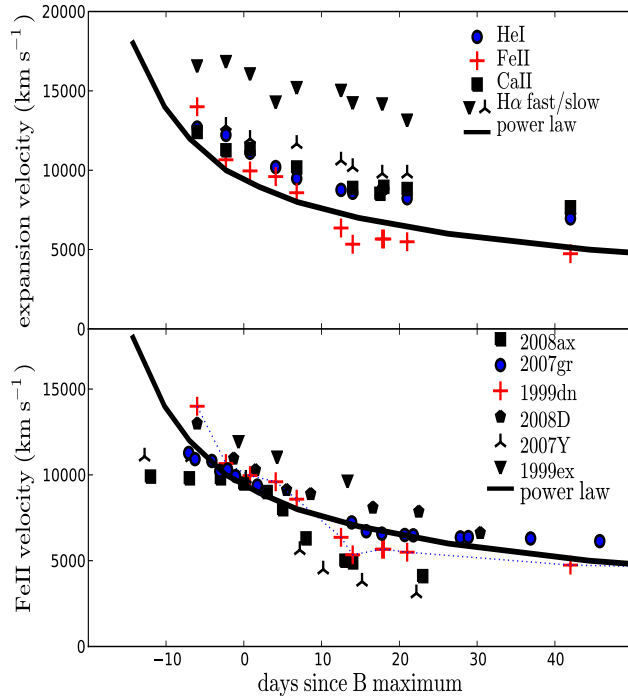


**Figure 9.** Top panel: velocity evolution of the HeI, FeII, CaII IR and H $\alpha$  lines of SN 1999dn in the photospheric phase. The crosses are the averages of the velocities derived from the minima of FeII lines, adopted as indicators of the photospheric velocity; the circles the average velocities of HeI lines; the triangles (starred triangles) the velocity of the *fast* (*slow*) component of H $\alpha$ , and the squares the velocity of the CaII IR triplet. Bottom panel: comparison of the velocity evolution of the FeII lines in several SE SNe. In both panels the curve is the power-law fit from Branch et al. (2002).

an expansion velocity smaller than SN 1999ex, but higher than other objects, e.g. SN 2007Y. Only at early phases the velocity seems to deviate from the power-law fit by Branch et al. (2002). At these early phases the expansion velocity is, in fact, more similar to that shown by the energetic SN 2008D. The overall normal velocity behavior indicates that the broad (slowly evolving) light curve of SN 1999dn after the peak is probably not due to a low expansion velocity but to a larger ejected mass.

#### 4.2 SN 1999dn and other Stripped Envelope SNe

We have compared the spectra of SN 1999dn with those of other SNe by means of GELATO, the spectra comparison tool developed by Harutyunyan et al. (2008) which compares input spectra with those present in our archive. Not unexpectedly, the best match is always with those of other SE SNe. In Fig. 10 we show the comparison with a number of well studied objects during the pre-maximum and maximum phase. At these epochs the objects that match SN 1999dn best are the extensively studied SNIb SN 2008ax (Pastorello et al. 2008; Chornock et al. 2010; Taubenberger et al. 2010) and the energetic SN 2008D (Mazzali et al. 2008; Modjaz et al. 2009).

For the first spectrum of SN 1999dn (−6d) the closest match is with SN 2008ax on days −9 and −8 (Pastorello et al. 2008; Taubenberger et al. 2010). The strong H $\alpha$ , which unequivocally marks the presence of H in SN 2008ax at this epoch, corresponds in position to the 6200 Å feature of SN 1999dn. Note, however, that the spectra of SN 2008ax that best match those of SN 1999dn are at an earlier phase, probably because of a faster expansion velocity of SN 1999dn. At this epoch, the numerical match with is poorer because its expansion velocity at such epoch is even higher (Mazzali et al. 2008). There is also a general resemblance to SN 2007Y, but the expansion velocity of SN 1999dn is significantly larger.

Also at maximum SN 1999dn best matches and SN 2008ax before their B maxima. The SED of SN 1999dn, however, is slightly redder. The 6200 Å feature corresponds to the fast blue wing of the H $\alpha$  absorption of SN 2008ax.

The comparison after maximum is shown in Fig. 11. On day +12.5 (top) the spectra of all objects are very similar. While H $\alpha$  in SN 2008ax is still very strong, the 6200 features of both SN 1999dn and SN 2007Y have dimmed and two notches are left where the broad absorption was before (cfr. Fig. 7). Again, due to smaller expansion velocity (cfr. Fig. 9), the absorptions in SN 2007Y are redder than in SN 1999dn.

A late-time (371d) red-grism spectrum has been obtained for SN 1999dn (Fig. 11 bottom). In both SN 2008ax and SN 2007Y, a broad shoulder on the red edge of [OI]  $\lambda\lambda 6300, 6364$  is clearly visible, which might be interpreted as a sign of interaction of a fast ( $v \sim 10000 \text{ km s}^{-1}$ ) shell with circumstellar material. However, the late time interaction scenario is not fully consistent and other interpretations have been proposed, though not proved (cfr. Taubenberger et al. 2010). At the same position only unresolved H $\alpha$ , [NII] and [SII] lines from an underlying HII region are discernible in SN 1999dn, a sign that there is not (yet) CSM interaction. [OI]  $\lambda\lambda 6300, 6364$  and [CaII]  $\lambda\lambda 7191, 7323$  ([OII]  $\lambda\lambda 7300, 7330$ ) are clearly visible, with a [CaII]/[OI] flux ratio of  $0.55 \pm 0.10$ .

## 5 DISCUSSION

SN 1999dn was extensively studied in the last decade but our new data allow a better determination of the main parameters (cfr. Tab. 4). The light curve results to be 0.5 mag brighter ( $M_V = -17.2$ ) than previously estimated, but still fainter than the average of SNIb/c ( $M_V = -17.70$ ,  $H_0 = 72 \text{ km s}^{-1} \text{ Mpc}^{-1}$ , Richardson, Branch, & Baron 2006). The multicolor observations (Sect. 3) have shown a relatively strong NIR flux. This large NIR flux is intrinsic, since the EW(NaID), the broad band colors and the SED all suggest SN 1999dn to be only mildly reddened ( $E(B-V) = 0.1$ , cfr. Sect. 3.1). The NIR accounts for about 50% of the flux during the advance photospheric phase. The bolometric light curve reaches the same luminosity as SNe 2007gr and 1999ex, but is brighter than SN 2007Y, and has a width similar to that of SN 2004aw (cfr. Fig. 5). It is known that the peak luminosity gives hints on the ejected  $^{56}\text{Ni}$  mass, while the width carries information on the total mass of the ejecta and kinetic energy. To extract in a self consistent manner information on the ejected mass ( $M_{ej}$ ), the nickel mass, ( $M(^{56}\text{Ni})$ ), and the kinetic energy ( $E_K$ ), we have em-

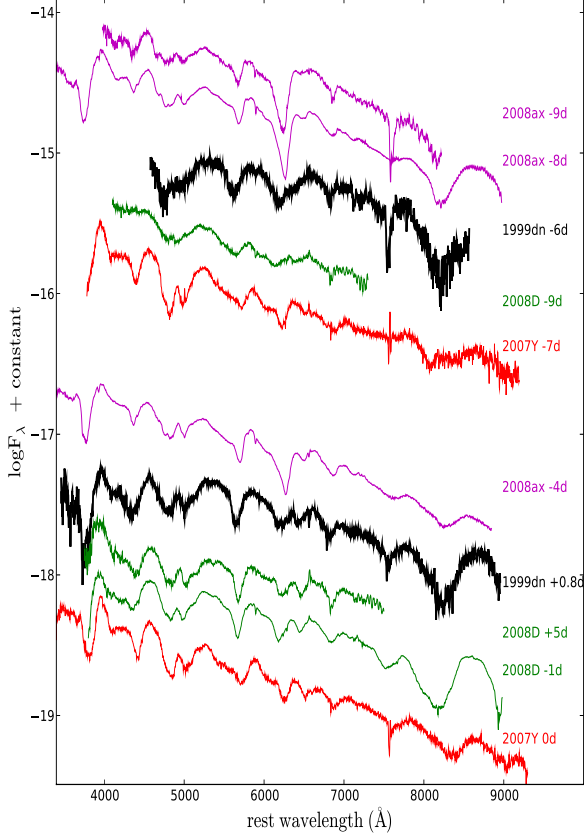


**Figure 10.** Comparison of the pre-maximum (−1 week, top) and maximum-light (bottom) spectra of SN 1999dn with those of other SE SNe. The spectra are plotted in the SN restframe and dereddened according to Tab. 5. The phase relative to the B maximum of each object is reported close to the SN identifier. The spectra come from Mazzali et al. (2008) and Valenti et al. (2011) for , from Pastorello et al. (2008) and Taubenberger et al. (2010) for SN 2008ax, from Stritzinger et al. (2009) for SN 2007Y, and from Deng et al. (2000) and this paper for SN 1999dn.

ployed a toy model of the bolometric light curve (Valenti et al. 2008b). Our procedure is based on a two-component analytical model to account for the photospheric and nebular phases. During the photospheric phase ( $t \leq 30$  d past explosion) a homologous expansion of the ejecta, spherical symmetry, and a concentration of the radioactive  $^{56}\text{Ni}$  exclusively in the core are assumed (Arnett 1982). At late times ( $t \geq 60$  d past explosion), the model includes the energy contribution from the  $^{56}\text{Ni}$ – $^{56}\text{Co}$ – $^{56}\text{Fe}$  decay, following the works of Sutherland & Wheeler (1984) and Cappellaro et al. (1997). The incomplete trapping of  $\gamma$ -rays and positrons has been accounted for using the Clocchiatti & Wheeler (1997) prescriptions for both photospheric and nebular phases. The bolometric light curve model suggests a  $^{56}\text{Ni}$  mass  $M(^{56}\text{Ni}) = 0.11 M_{\odot}$ . A comparison with the values from Table 2 of Hunter et al. (2009), obtained with similar methods, shows indeed that  $M(^{56}\text{Ni})$  is marginally larger than in SN 2007gr ( $0.076 M_{\odot}$ ), and SN 2007Y ( $0.06 M_{\odot}$ ),

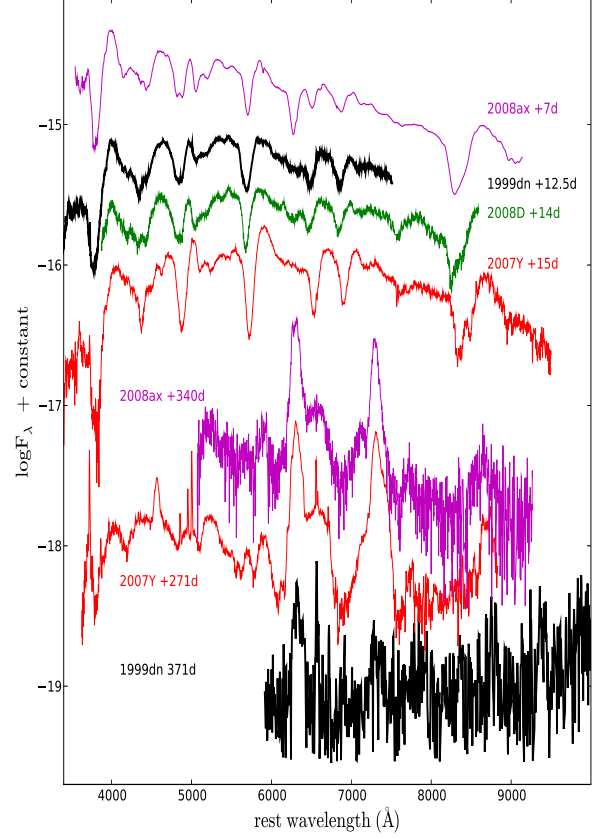


**Figure 11.** As in Fig. 10 but about 2 weeks (top) and 1 year (bottom) post-maximum. The spectra come from Modjaz et al. (2009) for , Taubenberger et al. (2010) for SN 2008ax, Stritzinger et al. (2009) for SN 2007Y and this paper for SN 1999dn.

Stritzinger et al. 2009), but smaller than 2004aw ( $0.3 M_{\odot}$ ). Using an average opacity of  $0.06 \text{ g/cm}$  (as in Valenti et al. 2008b) and a scale velocity  $v_{sc} = v_{ph} = 10100 \text{ km s}^{-1}$ , we obtain an ejected mass  $M_{ej} = 4 - 6 M_{\odot}$  and kinetic energy  $E_K = 5.0 - 7.5 \times 10^{51} \text{ erg}$ . **Surprisingly, but not totally unexpected because of the broadness of bolometric light curve of SN 1999dn, these values are comparable to those obtained for the energetic SN 2008D associated to an X-ray flash (Mazzali et al. 2008).** In fact our toy model makes use of the scale velocity of the explosion ( $v_{sc} = v_{ph}$ , which are similar for SNe 1999dn and 2008D) without taking into account possible differences in the density profiles.

In the case of SN 1999dn this may cause an overestimate of the physical parameters, the real values being at the lower boundary of those ranges. A more precise determination should rely on more detailed codes. A comparison between the physical parameters deduced, for a sample of well studied SNIb, with our toy model with those derived by more sophisticated codes will be given in Valenti et al 2010 (in preparation). Anyway, even considering the pos-

sibility that some physical values for SN 1999dn are slightly over-estimate, the supernova seems to belong to the group of relatively massive and energetic SNe Ib.

We noticed in Sect. 4.1 that the evolution of the photospheric velocity of SN 1999dn (as well as those of HeI and H) are in general very similar to those of other SNIb which implies, following Branch et al. (2002), comparable density profiles, masses and kinetic energies above the photospheres. As noticed by those authors, the strong similarity does not leave much room for asymmetries in SNIb, which is confirmed by the [OI] line profile of SN 1999dn at late time (Taubenberger et al. 2009). Only the earliest (−6d) measurement of the FeII velocity is significantly larger than the power law fit by Branch et al..

The previously available spectra of SN 1999dn before and after maximum light have been extensively modeled by means of both the highly parametrized SYNOW (Deng et al. 2000; Branch et al. 2002) and the more sophisticated non-LTE PHOENIX codes (Ketchum, Baron, & Branch 2008; James & Baron 2010). The latter successfully reproduces all main features of the spectra with a homogeneous stellar atmosphere of H, He, C, N, Ne, Na, Mg, Si, Ca and Fe with the main features identified as HeI, OI, CaII and FeII at all epochs. Also the HeI absorptions were successfully reproduced including  $\gamma$ -ray deposited by the radioactive  $\beta$  decay of  $^{56}\text{Co}$ .

Our new spectra confirm the presence of evolving features around 6200 Å during the first weeks (Sect. 4). Up to maximum light the region is dominated by a broad and strong feature which, if attributed to H, implies expansion velocities of about 17000 km s<sup>−1</sup> (cfr. Sect. 4.1 and Fig. 7). At subsequent epochs (days +6.8 to +21) our new, superior quality spectra confirm the presence of minor features (cfr. Ketchum, Baron, & Branch 2008) in the same region. Whether these components are due to H is not clear but the detection in the highest signal-to-noise spectra of weak absorptions at the same velocities with respect to H $\beta$  seems to support the existence of two H layers, one detached at velocities  $v = 17000$  to 13000 km s<sup>−1</sup>, comparable to that of H in other SNIb (Branch et al. 2002), the other only marginally faster than HeI ( $\Delta(v) \sim 1500$  km s<sup>−1</sup>, cfr. Fig. 9) and possibly located in the outer He layer. The high FeII velocity at the earliest epoch (−6d) seems compatible with the existence of high-velocity H-rich layers.

SN 2007Y and other SNIb show evidence of interaction of the fast expanding H-rich layer with the CSM (Fig. 11, bottom) about one year past maximum light. This is not the case in SN 1999dn, indicating that no major mass loss episodes have occurred in the last decade before the explosion (assuming wind velocities  $\sim 2000$  km s<sup>−1</sup>, typical of WR progenitors). There is also no evidence of dust formation at any time, neither from photometric (light and color curves) nor from spectroscopic observations (line positions and shapes).

On the spectrum obtained at WHT on Sept. 9, 1999, we have measured the O3N2 index (Pettini & Pagel 2004) of the region adjacent to SN 1999dn along the slit of the spectrograph, corresponding to projected linear distance of  $\sim 200$  pc at the adopted distance of the SN. Relation (3) of Pettini & Pagel (2004) thus provides an oxygen abundance at the SN location  $12 + \log(O/H) = 8.39 \pm 0.25$  (the er-

ror is the 95% spread of the calibrating relation) marginally lower than the solar abundance  $12 + \log(O/H) = 8.69 \pm 0.05$  (Asplund et al. 2009) and close to the average metallicity derived for the sites of a sample of fifteen SNIb, which includes also SN 1999dn, studied in Modjaz et al. (2010).

A search for the progenitor of SN 1999dn has been carried out on HST archive images (Van Dyk et al. 2003). The progenitor was not detected down to  $M_V \geq -7.3$  mag and  $(U-V)_0 \leq 2.5$  mag (these values do not change significantly with our assumptions on  $H_0$  and  $E(B-V)$ ). Unfortunately this determination does not strongly constraints the nature of the progenitor either as a massive, single WR star (e.g.  $M_{\text{ZAMS}} \geq 23 - 25 M_\odot$  at  $Z=0.02$ , Georgy et al. 2009), or as a star of lower initial mass in an interacting binary system (e.g.  $M_{\text{ZAMS}} \geq 14 - 16 M_\odot$  at  $Z=0.02$ , Yoon, Woosley, & Langer 2010). However the lack of signatures of dust favors the single, massive star scenario, given the fact that while the radiation field of single WR stars is expected to prevent dust formation in their local environment, while binarity in WR stars seems to provide the necessary physical conditions for it (Crowther 2007, and references therein).

The relatively high-metallicity environment ( $12 + \log(O/H) \sim 8.4$  corresponding to an almost solar,  $Z=0.02$ , metallicity) in which SN 1999dn exploded seems to support the single scenario. In fact, the binary channel for producing WR stars in WR galaxies (as NGC 7714) is important just at lower ( $12 + \log(O/H) < 8.2$ ) metallicity (e.g. Lopez-Sanchez & Esteban 2010), while the probability of forming single WR stars increases with the metallicity because it is easier to reach the WR phase due to the metallicity-dependence of the stellar wind (e.g. Lopez-Sanchez & Esteban 2010, and references therein). The lower mass limit for having a WR progenitor decreases from  $\sim 40 - 50 M_\odot$  at  $Z=0.004$  to  $\sim 23 - 25 M_\odot$  at  $Z=0.02$  (Georgy et al. 2009). As a consequence the progenitor of SN 1999dn is likely a single WR star having a main sequence mass  $\geq 23 - 25 M_\odot$ .

Also the relatively small flux ratio  $[\text{CaII}]/[\text{OI}] = 0.55 \pm 0.10$ , known for being constant with time (cfr. the spectra collection by Taubenberger et al. 2009) is consistent with a single massive star scenario. In fact, Fransson & Chevalier (1987, 1989) have shown that this ratio is a diagnostic of the core mass of the progenitor, with higher ratios indicative of smaller cores. The ratios measured for SN 1993J, SN 2007Y and SN 2008ax are 0.6, 1.0 and 0.9, respectively (Stritzinger et al. 2009; Taubenberger et al. 2010). Since the core mass is strongly dependent on the progenitor ZAMS mass, thus we have an indication that the progenitor of SN 1999dn is more massive than the above mentioned SNe.

## 6 CONCLUSIONS

We have presented detailed photometric observations and new spectra of SN 1999dn from before maximum to the nebular phase. These new data turn this object, already considered a prototypical SNIb, into one of the best observed objects of this class.

SN 1999dn was a moderately faint SNIb ( $M_V = -17.2$  mag) which produced 0.11  $M_\odot$  of  $^{56}\text{Ni}$ . With a toy model we have estimated an ejected mass of 4–6  $M_\odot$  with  $E_K = 5.0 - 7.5 \times 10^{51}$  erg. Due to the rough approximation of the model, these values may be slightly over-estimated. Our

analysis on SN 1999dn confirms that, contrary to early belief, a prototypical SN Ib may produce several foe of kinetic energy and eject several solar masses.

Overall the main parameters of the explosion are comparable to those of the type Ic SN 2004aw and the massive type Ib, much higher than those of the low-energy and low-ejected-mass SN 2007Y. Higher explosion energy and ejected mass, along with the small flux ratio  $[\text{CaII}]/[\text{OI}]$ , the lack of signatures of dust formation and the relatively high-metallicity environment point toward a single massive progenitor ( $M_{\text{ZAMS}} \geq 23-25 M_{\odot}$ ). On the other hand, none of these evidences completely rule out the scenario of a less massive star in a binary system.

The spectra of SN 1999dn at various epochs are similar to those of other SE SNe that show clear presence of H at early (type IIb SNe 1993J and 2008ax, type Ib SNe 2000H, 2007Y and 1999ex) or late (SNe 1993J, 2008ax, 2007Y) epochs. Such similarities, coupled to the fact that accurate spectral modeling (e.g. Ketchum, Baron, & Branch 2008) did not find other satisfactory explanations for the puzzling 6200Å feature, lead us to support its identification with detached H $\alpha$ . We conclude, therefore, that it is likely that residual H can be recognized in the spectra of most SNIb if observed sufficiently early on.

## ACKNOWLEDGMENTS

The SN 1999dn spectra published by Deng et al. (2000) and Matheson et al. (2001) have been retrieved from the Suspect database (

<http://bruford.nhn.ou.edu/~suspect/index1.html>

). We acknowledge the usage of the HyperLeda database (

<http://leda.univ-lyon1.fr>

)

We thank the referee, Chornock, R., for his helpful comments. SB, MT, EC and FB are partially supported by the PRIN-INAF 2009 with the project "Supernovae Variety and Nucleosynthesis Yields".

## REFERENCES

- Anderson, J.P., James, P.A. 2008, MNRAS, 390, 1527  
 Arnett W.D., 1982, ApJ, 253, 785  
 Asplund M., Grevesse N., Sauval A. J., Scott P., 2009, ARA&A, 47, 481  
 Ayani, K., Furusho, R., Kawakita, H., Fujii, M., Yamaoka, H., 1999, IAUC 7244, 1  
 Barbon R., Benetti S., Cappellaro E., Patat F., Turatto M., Iijima T., 1995, A&AS, 110, 513  
 Branch D., et al., 2002, ApJ, 566, 1005  
 Cappellaro E., Mazzali P. A., Benetti S., Danziger I. J., Turatto M., della Valle M., Patat F., 1997, A&A, 328, 203  
 Chevalier, R. A., & Soderberg, A. M. 2010, ApJL, 711, L40  
 Chornock R., et al., 2010, arXiv:1001.2775  
 Clocchiatti A., Wheeler J. C., Brotherton M. S., Cochran A. L., Wills D., Barker E. S., Turatto M., 1996, ApJ, 462, 462  
 Clocchiatti, A., Wheeler, J.C. 1997, ApJ, 491, 375  
 Crowther P. A., 2007, ARA&A, 45, 177  
 Deng, J.S., Qiu, Y.L., Hu, J.Y., Hatano, K., Branch, D., 2000, ApJ 540, 452  
 Desroches, L.B., Wang, X., Ganeshalingam, M., Filippenko, A., 2007, CBET 1001  
 Dessart L., et al., 2008, ApJ, 675, 644  
 Elmhamdi A., Danziger I. J., Cappellaro E., Della Valle M., Gouiffes C., Phillips M. M., Turatto M., 2004, A&A, 426, 963  
 Filippenko A. V., 1982, PASP, 94, 71  
 Filippenko A. V., et al., 1995, ApJ, 450, L11  
 Fransson C. & Chevalier R., 1989, ApJ, 343, 323  
 Fransson C. & Chevalier R., 1987, ApJ, 322, 15  
 Freedman W. L., et al., 2001, ApJ, 553, 47  
 Folatelli G., et al., 2006, ApJ, 641, 1039  
 Fynbo J.P.U., et al., 2004, ApJ, 609 962  
 Galama T. J., et al., 1998, Nature, 395, 670  
 Georgy C., Meynet G., Walder R., Folini D., Maeder A., 2009, A&A, 502, 611  
 Hakobyan A. A., Petrosian A. R., McLean B., Kunth D., Allen R. J., Turatto M., Barbon R., 2008, A&A, 488, 523  
 Hamuy M., et al., 2002, AJ, 124, 417  
 Harutyunyan A. H., et al., 2008, A&A, 488, 383  
 Heger A., Fryer C. L., Woosley S. E., Langer N., Hartmann D. H., 2003, ApJ, 591, 288  
 Hjorth J., et al., 2003, Nature, 423, 847  
 Hunter, D. et al, 2009, A&A, 508, 371  
 James, S. & Baron, E., 2010, ApJ, 718, 957  
 Kandrika, H., Li, W., 2007, CBET 997  
 Ketchum W., Baron E., Branch D., 2008, ApJ, 674, 371  
 Kraan-Korteweg R. C., 1995, yCat, 7098, 0  
 Landolt, A.U., 1992, AJ 104, 340  
 Li, W. et al., 2010, MNRAS submitted, arXiv:1006.4612  
 Lopez-Sanchez A. R., Esteban C., 2010, arXiv:1004.0051  
 Malesani D., et al., 2004, ApJ, 609, L5  
 Matheson, T., Filippenko, A.V., Li, W., Leonard, D.C., 2001, ApJ 121, 1648  
 Mattila S., Meikle P., Walton N., Greimel R., Ryder S., Alard C., Lancon A., 2002, IAUC, 7865, 2  
 Mazzali P. A., et al., 2008, Sci, 321, 1185  
 Modjaz M., et al., 2006, ApJ, 645, L2  
 Modjaz M., et al., 2009, ApJ, 702, 226  
 Modjaz M., et al., 2010, ApJL, submitted, arXiv:1007.0661v1  
 Pastorello, A., Turatto, M., Rizzi, L., Cappellaro, E., Benetti, S., Patat, F., 1999, IAUC 7245  
 Pastorello A., et al., 2008, MNRAS, 389, 955  
 Pettini M., Pagel B. E. J., 2004, MNRAS, 348, L59  
 Pian E., et al., 2006, Nature, 442, 1011  
 Qiu, Y.L., Qiao, Q.Y., Hu, J.Y., 1999, IAUC 7241  
 Qiu, Y.L., Huang, I., Yao, B., Li, H., 1999, IAUC 7244  
 Roming, P. W. A., et al., 2009, ApJL, 704, L118  
 Richardson D., Branch D., Baron E., 2006, AJ, 131, 2233  
 Richmond M. W., et al., 1996, AJ, 111, 327  
 Richmond M. W., Treffers R. R., Filippenko A. V., Paik Y., 1996, AJ, 112, 732  
 Schlegel, D.J., Finkbeiner, D.P., Davis, M., 1998, ApJ 500, 525  
 Soderberg A. M., et al., 2008, Nature, 453, 469  
 Stritzinger M., et al., 2002, AJ, 124, 2100  
 Stritzinger M., et al., 2009, ApJ, 696, 713

- Skrutskie M. F., et al., 2006, AJ, 131, 1163  
Sutherland P. G., Wheeler J. C., 1984, ApJ, 280, 282  
Taubenberger, S., et al., 2006, MNRAS, 371, 1459  
Taubenberger, S., et al., 2009, MNRAS, 397, 677  
Taubenberger, S., et al., 2010, MNRAS, submitted  
Turatto, M., Rizzi, L., Salvo, M., Cappellaro, E., Benetti, S., Patat, F., 1999, IAUC 7244  
Turatto M., Benetti S., Cappellaro E., 2003, fthp.conf, 200  
Turatto M., Benetti S., Pastorello A., 2007, AIPC, 937, 187  
Valenti S., et al., 2008, ApJ, 673, L155  
Valenti S., et al., 2008, MNRAS, 383, 1485  
Valenti S., et al., in preparation  
Van Dyk S. D., Peng C. Y., Barth A. J., Filippenko A. V., 1999, AJ, 118, 2331  
Van Dyk S. D., Li, W., Filippenko A. V., 2003, PASP, 115, 1  
Weedman, D.W., Feldman, F.R., Balzano, V.A., et al., 1981, ApJ 248, 105  
Wheeler J. C., Levreault R., 1985, ApJ, 294, L17  
Woosley S. E., Eastman R. G., 1997, thsu.conf, 821  
Yoon S.-C., Woosley S. E., Langer N., 2010, arXiv:1004.0843